J Mol Med (2008) 86:999–1011
DOI 10.1007/s00109-008-0379-2

ORIGINAL ARTICLE

In vivo dendritic cell depletion reduces breeding efficiency, affecting implantation and early placental development in mice

Gesa Krey · Pierre Frank · Valerie Shaikly · Gabriela Barrientos · Rosalia Cordo-Russo · Frauke Ringel · Petra Moschansky · Igor V. Chernukhin · Metodi Metodiev · Nelson Fernández · Burghard F. Klapp · Petra C. Arck · Sandra M. Blois

Received: 28 November 2007 / Revised: 2 June 2008 / Accepted: 9 June 2008 / Published online: 25 June 2008

Abstract Implantation of mammalian embryos into their mother's uterus ensures optimal nourishment and protection throughout development. Complex molecular interactions characterize the implantation process, and an optimal synchronization of the components of this embryo-maternal dialogue is crucial for a successful reproductive outcome. In the present study, we investigated the role of dendritic cells (DC) during implantation process using a transgenic mouse system (DTRtg) that allows transient depletion of $CD11c^+$ cells in vivo through administration of diphtheria toxin. We observed that DC depletion impairs the implantation process, resulting in a reduced breeding efficiency. Furthermore, the maturity of uterine natural killer cells at dendritic cell knockout (DCKO) implantation sites was affected as well; as demonstrated by decreased perforin expression and reduced numbers of periodic-acid-Schiff (PAS)-positive cells. This was accompanied by disarrangements in decidual vascular development. In the present study, we were also able to identify a novel DC-dependent protein, phosphatidylinositol transfer protein β (PITPβ), involved in implantation and trophoblast development using a proteomic approach. Indeed, DCKO mice exhibited substantial anomalies in placental development, including hypocellularity of the spongiotrophoblast and labyrinthine layers and reduced numbers of trophoblast giant cells. Giant cells also downregulated their expression of two characteristic markers of trophoblast differentiation, placental lactogen 1 and prolifferin. In view of these findings, dendritic cells emerge as possible modulators in the orchestration of events leading to the establishment and maintenance of pregnancy.

Keywords Dendritic cells · Implantation · Natural killer cells · Placentation

Pierre Frank and Valerie Shaikly contributed equally to this work.

G. Krey · P. Frank · G. Barrientos · R. Cordo-Russo · F. Ringel · P. Moschansky · B. F. Klapp · P. C. Arck · S. M. Blois (✉)
Charité Centrum 12 für Innere Medizin und Dermatologie,
Reproductive Immunology Research Group,
University Medicine of Berlin,
BMFZ-Raum 2.0547, CVK, Augustenburger Platz 1,
13353 Berlin, Germany
e-mail: sandra.blois@charite.de

V. Shaikly · I. V. Chernukhin · M. Metodiev · N. Fernández
Department of Biological Sciences, University of Essex,
Wivenhoe Park,
Colchester C04 3SQ, UK

Introduction

In mammals, the evolutionary adaptation that allows implantation of the blastocyst in the mother's uterus ensures optimal nourishment and protection of the fetus throughout its entire development. However, this arrangement also creates a threatening situation, since the intimate juxtaposition of fetal and maternal cells provides a prospect for the development of maternal immune responses against fetal 'semi-allogeneic' tissue. Yet, despite genetic differences, mothers do not reject their semi-allogeneic embryos, and many hypotheses have been proposed to explain the immunologically privileged status of the feto-placental unit [1].

Evidence published to date reveals that implantation involves complex molecular interactions between mature blastocysts and the hormonally primed uterus. Although

comparatively little is known about the hierarchy of events involved, failure to synchronize the components of this dialogue results in a failure of implantation. In mice, the initial attachment between the blastocyst and the luminal epithelium occurs on gestation day (Gd) 4.5 and coincides with increased stromal vascular permeability and secretory activity of endometrial glands. This is followed by stromal cell proliferation and differentiation (decidualization) at the sites of blastocyst apposition [2, 3]. Of the many aspects involved in the implantation process, the role of ovarian steroid hormones is probably the best understood. Progesterone (P4) appears to be an absolute requirement for decidualization since progesterone receptor (*Pgr*)-deficient mice fail to exhibit decidualization, while estrogen receptor 1 (*Esr1*)-deficient mice can respond to deciduogenic stimuli only in the presence of P4 [4].

Although the most obvious feature of decidualization is the stromal cell transformation, there are distinctive changes in all elements of the endometrium, including endometrial glands, arteries, and leukocytes. During early pregnancy, the uterine mucosa of both mice and humans is strikingly enriched with leukocytes belonging to the natural killer cell lineage. Indeed, such uterine natural killer (uNK) cells dramatically increase their numbers post-ovulation and peak at the time of decidualization when they constitute around 70% of uterine leukocytes [5]. The maturation of uNK cell precursors in the decidua appears to be mostly driven by IL-15 [6, 7] produced by dendritic cells, other leucocytes, and epithelial cells [6, 8, 9] and renders large granulated cells bearing high levels of cytolytic mediators (i.e., perforin and granzymes). It has been suggested that uNK cells may play a role in the regulation of maternal mucosal and arterial function [6] and/or trophoblast invasion [10]. In particular, uNK cell-derived interferon gamma (IFN-γ) has been found to be essential for pregnancy-induced vascular remodeling in mice [11]. Given that uNK cells are the predominant leukocyte population at the onset of decidualization, these cells are also most likely to influence this process. Indeed, this is reflected by the finding that mouse strains lacking uNK cells exhibit hypocellular and edematous decidua basalis and thickening of the arterial walls with persistence of vascular smooth muscle and luminal narrowing [12]. Interestingly, implantation in these mouse strains is normal, and fetal loss (when observed) coincides with the detection of placental defects around Gd 10.5 [13].

Although several studies have shed light into the regulatory functions of uNK cells in the implantation process, the contribution of other leukocyte populations remains largely elusive. Recent evidence suggests that dendritic cells (DC) may also perform regulatory functions at the maternal fetal interface [14]. Indeed, it has been shown that DC increase their numbers at the peri-implantation period, namely on Gd 5.5 in mice [14]. This increase was accompanied by a transitory decrease in the relative number of DC producing the Th2 cytokine interleukin 10 (IL-10). Although successful pregnancy is widely recognized as a Th2 phenomenon, it is well established that an inflammatory milieu involving several Th1 cytokines mediates the communication between embryonic cells and maternal uterine cells as part of the physiologic response to implantation [15, 16]. A cross talk between uterine DC and uNK cells at the feto-maternal interface is also likely to be important for pregnancy [17]. Early studies have provided valuable clues into such DC-NK cell cross talk in the periphery by describing the following interactions: (1) production of IL-15, IL-12/IL-18, and type I IFN by mature DC induces proliferation, IFN-γ secretion, and cytotoxic functions of NK cells [18, 19]; (2) activated NK cells can induce DC maturation [20]; and finally, (3) immature DC are susceptible to NK-cell-mediated cytolysis. More recently, our studies in mice showing that interactions between DC and uNK cells influence uterine cell proliferation in vitro bring special emphasis to the role played by these cell subsets in the delicate signaling network at the fetal–maternal interface [21]. In view of these findings, the aim of the present study was to investigate the role of DC during the implantation process in mice.

Materials and methods

Animals

B6.FVB-Tg$^{CD11c\text{-}DTR/EGFP.57}$Lan/J mice (referred to as DTRtg mice) were purchased from Jaxmice® and maintained in an animal facility with a 12L/12D cycle. Animal care and experimental procedures were followed according to institutional guidelines and conformed to requirements of the state authority for animal research conduct (LaGeSo, license G0037/06, Berlin). After overnight cohabitation with Balb/c males, DTRtg or wild-type C57BL/6 females with vaginal plugs (which equals Gd 0.5) were separated from males, injected intraperitoneally with 4 ng/g body weight diphtheria toxin [DT; in phosphate buffered saline (PBS); Sigma-Aldrich, Germany] or PBS 200 μl on Gd 4.5, and assigned to three different groups and killed on Gd 5.5, 7.5, 10.5, or 13.5 (n=5 each Gd/per group). DTRtg mice treated with DT are referred to as dendritic cell knockout (DCKO) mice.

Tissue collection

Uterine cells were isolated using our standard protocol [12]. Lymph nodes and spleens were carefully dissected and harvested in sterile PBS, pressed through a 100-μm syringe, and washed twice with PBS followed by flow cytometric analysis.

Blood sampling

On gestation days 5.5 and 13.5, mice from the respective groups were narcotized, and blood was obtained by retro-orbital puncture and collected in tubes containing heparin. After treatment with ammonium chloride lysis buffer for 10 min to deplete erythrocytes, blood cells were washed twice with sterile PBS and thereafter used for analysis by flow cytometry. For serum sampling, blood was collected in heparin-free tubes. After centrifugation, the clear supernatant was collected and stored at −80°C.

Flow cytometric analysis

Flow cytometry was performed using our standard protocol [12]. Briefly, blood, spleen, inguinal lymph nodes, or uterus cells were washed twice with FACS buffer [PBS supplemented with 1% bovine serum albumin (BSA; Sigma-Aldrich)] and 0.1% sodium azide (Sigma-Aldrich). Cells were then incubated 30 min at 4°C with previously optimized amounts of the fluorescein-isothiocyanate-conjugated murine monoclonal antibody against integrin alpha X (CD11c; Miltenyi Biotec, Germany). Two percent of normal mouse serum was added to avoid non-specific binding by Fc receptors. As a control, cells were stained with the corresponding isotype-matched mAb. The cells were then washed and read. The acquisition was performed using a FACSCalibur (BD Biosciences, Germany). Instrument compensation was set in each experiment using single-color stained samples. Data were analyzed with CellQuest software. Flow cytometry results were expressed as the percentage of cells positive for the surface marker evaluated.

Semi-quantitative reverse transcriptase PCR

Total RNA was extracted from uterine tissues with Nucleospin RNA/protein isolation kit (Macherey-Nagel, Germany) following the manufacturer's instructions. After DNase digestion (Invitrogen, Germany), total RNA was reverse-transcribed with random primers (Invitrogen) followed by polymerase chain reaction (PCR) amplification for interleukin 15 (IL-15) and interleukin 15 receptor (IL-15R) using the following primers: IL-15 forward primer 5′-CAGTTGCA GAGTTGGACGAA-3′; IL-15 reverse primer 5′-GCAATT CCAGGAGAAAGCAG-3′; IL-15R forward primer 5′-GA GACCCCTCCCTAGCTCAC-3′; IL-15R reverse primer 5′-ATCGTGTGGTTAGGCTCCTG-3′ (all primers from Tib-Molbiol, Germany). PCR reactions were performed for 30 cycles with a denaturing temperature of 94°C (1 min), annealing temperature 60°C (1 min), extension temperature 72°C (1 min), followed by final extension at 72°C for 10 min. The sizes of the expected amplified products for IL-15 and IL-15R are 580 and 470 bp, respectively. As a control, a conventional PCR for hypoxanthine guanine phosphoribosyl transferase 1 (HPRT) was performed using the following primers: HPRT forward primer 5′-GTTGGATACAGGCCA GACTTTGT-3′; HPRT reverse primer 5′-CACAGGACTA GAACACCTGC-3′ (Tib-Molbiol). The size of the expected PCR product is 225 bp. PCR reactions were performed for 30 cycles with a denaturing temperature 94°C (1 min), annealing temperature 60°C (1 min), and extension temperature 72°C (1 min) followed by 10-min final extension at 72°C. All amplified products were separated by agarose gel electrophoresis (2%) and stained with ethidium bromide. Photo documentation was performed using the UV-transilluminator Eagle Eye II (Stratagene). Density of detected bands was quantified using Scion Image (Scion Corporation, Frederick, MD, USA).

H&E staining

Eight-micrometer tissue sections obtained from gestation day 10.5 were stained using our standard protocol. Briefly, samples were washed 5 min in Tris-buffered saline (TBS) buffer followed by incubation in Mayer's hematoxylin for 12 min at room temperature (RT). Slides were then washed in tap water for 15 min and incubated in eosin for 20 min. This was followed by dehydration through ethanol 100% (two times, 2 min each) and xylene (two times, 5 min each) and mounting in Vitro-Clud (R. Langenbrinck, Germany). Tissue sections were examined with a light microscope (Axiophot) and photographs taken with Axio Cam HRc. Photo documentation was performed using digital image analysis system Spot advanced software, version 4.6 (Visitron Systems).

Periodic acid Schiff staining on paraffin-embedded sections

Paraffin slides were treated with standard deparafinization and rehydration procedures: incubation in xylene 10 min, xylene 10 min, ethanol 100% 1 min, ethanol 100% 1 min, ethanol 96% 1 min, ethanol 80% 1 min, and ethanol 70% 1 min at RT.

Sections were incubated for 10 min at RT in 1% periodic acid followed by washing using tap water for two times 5 min. After incubation with Schiff reagent for 20 min at RT, the sections were washed using tap water twice for 5 min. All sections were counterstained by incubation in hematoxylin solution for 1 min at RT and washed 5 min in tap water. After that, sections were dehydrated by incubation with ethanol 70% 1 min, ethanol 80% 1 min, ethanol 96% 1 min, ethanol 100% 1 min, ethanol 100% 1 min, xylene 5 min, and xylene 5 min. Slides were mounted with Vitro-Clud (R. Langenbrinck). The stained tissue sections were examined with a light microscope (Axiophot) and pictures taken with Axio Cam HRc. Photo documentation was performed using digital image analysis system Spot advanced software, version 4.6 (Visitron Systems).

Separation of proteins by 2-DE

Uterine protein isolation for 2-DE

Uterine tissue was resuspended in 90 μl rehydration buffer (7 M urea, 2 M thiourea, 4% *w/w* CHAPS) containing 2 μl protease inhibitor (Sigma Aldrich) and homogenized with a pellet pestle rotor device for three times 1 min. Afterwards, the samples were rotated at 4°C for 20 min and centrifuged at 5,000×*g*. The supernatant was collected and total protein concentration determined by Bradford assay at 595 nm.

First dimension

The first dimension of 2D electrophoresis was performed on a Pharmacia Biotech Multiphor Electrophoresis System. Linear pH 3±10 Immobiline DryStrips were rehydrated overnight at room temperature in rehydration buffer [7 M urea, 2 M thiourea, 65 mM dithiothreitol (DTT), 4% *w/w* CHAPS, 0.6% carrier Pharmalyte pH 3±10]. Uterine proteins (70 μg) were applied during rehydration. The first dimension was run for 70,572 Vh (IPG-Phor Ettan) using the following conditions at 20°C: 200 V, 500 Vh; 500 V, 500 Vh; 1,000 V, 2,500 Vh; 8,000 V, 13,500 Vh; 8,000 V, 53,500 Vh; 500 V, 72 Vh. Next, gels were equilibrated for 15 min in buffer [6 M urea, 50 mM Tris–HCl pH 8.8, 30% glycerol, 2% sodium dodecyl sulfate (SDS), and 1% DTT].

Second dimension and protein staining

Uterine proteins from DTRtg, DCKO and wild-type mice were separated by denaturing SDS–polyacrylamide gel electrophoresis (SDS-PAGE) using Protean® II xi Cell (Bio-Rad, UK). Briefly, gel plates of 18×20 cm were assembled, and the plates were marked 2 cm from the top. Twelve percent resolving gel was poured up to the marked line, overlaid with 0.01% SDS, and left for 1 h to polymerize, after which, the 0.01% SDS solution was removed. After this, 2 ml of boiled agarose sealing solution was added and, immediately, the IPG strip overlaid. The run was performed at 250 V for 2–3 h and was stopped when the dye front was about 2 mm away from the bottom of the gel. Proteins were stained by the Silver Stain Plus® kit (Bio-Rad) following manufacturer's instructions. Development reaction was stopped by acetic acid 5% (*v/v*) when spots were clearly visualized. Gels were washed with abundant water and incubated overnight in an aqueous solution with glycerol 5% (*v/v*) and sodium azide 0.02% (*w/v*) for conservation. Finally, gels were imaged using an Epson expression 16000 Pro-Scanner and the software Epson scan.

In-gel trypsin digestion

To further explore the identity of the proteins present in each sample, the spots of interest were cut from the gels with disposable scalpels. The gel pieces were washed once with MilliQ (100 ml), and destained with 15 mM potassium ferricyanide/50 mM sodium thiosulfate. The samples were reduced with 10 mM DTT at 50°C for 30 min and then alkylated with 55 mM iodoacetamide for 60 min. The gel pieces were then dehydrated twice in 100% acetonitrile (ACN) for 10 min, dried in a SpeedVac, and then re-swollen with an in-gel digestion buffer containing 20 μg/ml sequencing grade trypsin (Promega, UK) in the 50 mM ammonium bicarbonate solution. The digestion was performed overnight at 37°C, and the tryptic peptides were extracted from the gel pieces and dried in a SpeedVac.

Protein identification using nano LC-MS/MS

The peptides were redissolved in 0.1% MS grade formic acid solution and then centrifuged at 10,000 rpm for 5 min. Samples were analyzed using Nano liquid chromatography/mass spectrometry/mass spectrometry (LC-MS/MS; Bruker® Esquire HCT).

Protein identification by peptide mass fingerprinting

The peptides were dissolved in 5 μl of 0.1% MS grade TFA, and 1 μl of each sample was spotted on a MALDI 384-well target plate and dried under vacuum. Matrix solution (1 μl; 10 mg/ml of α-cyano-4-hydroxycinnamic acid in 50% ACN, 0.1% TFA) was spotted on top of the previously applied digest and dried under vacuum. MS analysis of the samples was performed with matrix assisted laser desorption/ionization (MALDI) time-of-flight spectrometer (Bruker® Daltonics Reflex IV) in reflectron mode. The obtained spectra were interpreted using Bruker Daltonics flexAnalysis 2.0 software.

The resulting MS (MALDI) or MS/MS (LC-MS/MS) data were piped either to the peptide mass fingerprint or ion search engine, respectively, of locally installed Mascot server (http://www.matrixscience.com). The search was performed against the newly updated Uniprot (Swiss-Prot/TrEMBL) database. In both cases, the significance of the obtained results was estimated according to a Mowse score.

Immunoblotting

Total protein was extracted from uterine tissue at gestation day 5.5 using total protein extraction kit (Chemicon International). After centrifugation and collection of the supernatant, protein concentrations were determined by Bradford Assay (BioRad, Germany). Thirty micrograms of total protein was separated by SDS-PAGE under reducing conditions and were transferred onto polyvinylidene fluoride membranes (Amersham Biosciences, Germany). Blots were then incubated for 1 h in blocking solution (5% nonfat dry milk and 0.1% Tween 20 in PBS) followed by overnight

primary antibody incubation at 4° using goat polyclonal anti-PITP antibody (Santa Cruz, Germany, sc-20286) diluted 1:500 in 3% BSA/PBS. After washing with blocking solution, the blots were incubated with horseradish peroxidase-conjugated donkey-anti-goat IgG (Jackson ImmunoResearch, Germany) diluted 1:5,000 in 3% BSA/PBS. After washing with PBS, antibodies were detected by chemiluminescence with Western blotting luminal reagent (Santa Cruz) following manufacturer's instructions. Blots were stripped in stripping buffer (Chemicon, Germany) and re-probed using anti-actin beta (β-actin) antibody (Sigma-Aldrich, A2066) following the above protocol.

Immunofluorescence analysis

Sections (8 μm) were stained after the following protocol: washing in TBS buffer 3×5 min, blocking by incubation with 2% normal serum for 20 min at RT. Primary antibodies (ab) [anti-endoglin (sc-18893, 1/200), anti-platelet/endothelial cell adhesion molecule 1 (PECAM1, sc-18916, 1/200), anti-proliferin (PLF, sc-47345, 1/200), anti-placental lactogen 1 (PL-1, sc-34713, 1/400), anti-phosphatidylinositol transfer protein β (PITP, sc-20286, 1/100) all purchased from Santa Cruz Biotechnology except anti-cytokeratin polyclonal ab (Dako Cytomation, Germany, Z0622, 1/200)] were incubated overnight at 4°C. After washing in TBS buffer, sections were incubated with tetramethylrhodamine-isothiocyanate-conjugated secondary antibody (Jackson ImmunoResearch, Germany) for 1 h at RT. After washing in TBS buffer, sections were incubated in 4′,6-diamidino-2-phenylindole solution and again washed before mounting of slides. Negative controls with irrelevant IgG showed no specific immunoreactivity. Photo documentation was performed using digital image analysis system (Spot advanced software, version 4.6; Visitron Systems).

Immunohistochemistry

Staining of 8-μm sections was performed by washing in TBS buffer followed by blocking of endogenous peroxidase through incubation with 3% H_20_2 in methanol for 30 min at RT. After incubation with 2% normal serum for 20 min at RT, primary antibodies [anti-phospho H3 histone (PHH3) (sc-8656-R) and anti-Perforin 1 (sc-9105) purchased from Santa Cruz Biotechnology)] were added to the samples at previously optimized concentrations and incubated overnight. After washing in TBS buffer and incubation with peroxidase-conjugated secondary antibody (Jackson ImmunoResearch), sections were incubated with DAB substrate solution (Dako Cytomation) and washed with TBS buffer. Nuclei were counterstained with hematoxylin solution followed by standard dehydration procedure. Negative controls with irrelevant IgG showed no specific immunoreactivity. Photo documentation was performed using a digital imaging analysis system (Zeiss KS400).

Progesterone ELISA

To obtain steroid extracts from mice sera, extraction with diethylether was performed. Serum was mixed with diethylether (Merck, Germany) and rotated 15 min at 4°C. After vortexing and centrifugation 5 min at 3,000×*g*, the samples were incubated 20 min at −80°C to separate the organic phase. After concentrating by evaporation, the samples were processed in an ultrasound bath for 10 min. Steroid-free human serum (DRG, Germany) was added, and mixture was vortexed shortly and centrifuged 3 min at 3,800×*g*. After evaporation of the residing ether, samples were incubated in an ultrasound bath for 12 min followed by centrifugation 3 min at 3,800×*g*. The steroid extract was diluted 1:2 in steroid-free human serum before enzyme-linked immunosorbent assay (ELISA) application. Following steroid extraction from sera samples, a competitive ELISA was performed with a progesterone ELISA kit (DRG) to quantify progesterone concentration. In this solid-phase ELISA kit, the amount of bound peroxidase is reversely proportional to the concentration of progesterone in the sample, e.g., the intensity of color of the substrate solution is reversely proportional to the progesterone concentration in the serum sample. To perform the assay, 25 μl of each standard (0, 0.3, 1.25, 2.5, 5, 15, 40 ng/ml) and of each sample was loaded in the pre-coated wells. All samples and standards were measured in duplicates. Reading of the optical density occurred at 450 nm with a microtiter plate reader within 10 min after adding the stop solution. For the calculation of the results, the average absorbance values for each set of standard and sample was calculated, and a standard curve was constructed by plotting the mean absorbance obtained from each standard against its concentration. Using the mean absorbance value for each sample, the corresponding concentration was determined from the standard curve.

Statistical analysis

Statistical significance was determined using the nonparametric Mann–Whitney *U* test (Wilcox test). Significance was set at $P<0.05$.

Results

DT administration depletes $CD11c^+$ cells

The transgenic B6.FVB-$Tg^{CD11c\text{-}DTR/EGFP.57}$Lan/J mice express the DT receptor under transcriptional control of the CD11c promoter, which allows for selective depletion of DC following the administration of DT. In these mice, a single injection of DT efficiently depletes $CD11c^+$ cells [22].

These cells are detectable again 42 h after DT injection, reaching comparable numbers to non-injected mice after 66 h [23]. CD11c is expressed by all murine DC subsets except epidermal Langerhans cells. However, CD11c is also expressed by activated intraepithelial lymphocytes and $CD8^+$ LN T cells [22]. We first verified that DT causes depletion of DC, i.e., from the uterus, which would mimic the phenotype of a transient DC knockout (KO) in mice. As shown in Table 1, 24 h after DT administration, uteri were largely depleted of $CD11c^+$ DC. Moreover, $CD11c^+$ cells were also absent in blood, spleen, and inguinal lymph nodes from these mice. Since uterine DC were effectively depleted akin to KO mice (DCKO), we chose this model for the investigation of the role of DC during implantation.

Transient DC depletion causes an impaired implantation process

Since it is well known that uterine DC emerge during the peri-implantation period in mice [14], we tested the regulatory function of DC during implantation employing the DT-induced, short-term depletion of DC in vivo initiated on Gd 4.5 [22]. Assessment of the implantation sites revealed a significantly reduced number of implantations in DCKO mice (Fig. 1a). We have also observed a significant decrease on the breeding efficiency after DC depletion: while only 15 of 25 mice (60%) receiving DT injection had implantation, breeding efficiency in wild-type mice was 75%. Interestingly, PBS-treated transgenic mice (DTRtg) showed a higher breeding efficiency ratio (80%, Fig. 1b).

Table 1 Loss of $CD11c^+$ DC following DT administration

Mating combination	Tissue	Percentage of $CD11c^+$ DC
Wild-type mice	Uterus	8.56±0.90
DCKO		0.25±0.09**
DTRtg		7.22±0.83
Wild-type mice	Blood	6.95±0.52
DCKO		0.18±0.10**
DTRtg		5.85±0.78
Wild-type mice	Spleen	2.34±0.15
DCKO		0.12±0.08*
DTRtg		2.19±0.34
Wild-type mice	Inguinal lymph nodes	8.07±0.35
DCKO		0.24±0.12**
DTRtg		7.46±0.82

Percentages of $CD11c^+$ DC were assessed by flow cytometry after 24 h after DT administration in wild-type, DTRtg, and DC-depleted (DCKO) mice (n=5, per group). Results are expressed as mean±SEM. *P<0.01; **P<0.001 (as evaluated by non-parametric Mann–Whitney U test)

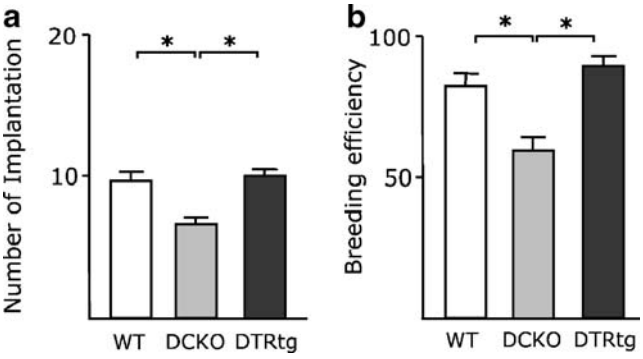

Fig. 1 Transient DC depletion impairs the implantation process in mice. **a** Number of implantations calculated by adding the normal implantation sites on gestation day 5.5 (n=6), 7.5 (n=5), and 10.5 (n=5). Data are depicted as the mean±SEM. *P<0.05 analyzed by non-parametric Mann–Whitney U test. **b** Breeding efficiency. For each group (wt vs. DCKO and DTRtg vs. DCKO), *bars* represent the mean percentage of pregnant mice± SEM; *P<0.05 analyzed by non-parametric Mann–Whitney U test

Effect of DC depletion on uterine NK cell differentiation, vascular organization, and decidualization

Based on the previously described spatial adjacencies of uterine NK cells and DC in human and mouse early pregnancy decidua [21, 24] and the role of IL-15 in the cross talk between these cell populations [18, 25], we decided to investigate whether DC depletion influences uterine IL-15 and IL-15R expression. At day 5.5 of pregnancy, IL-15 and IL-15R transcripts were detected in DCKO mice at similar levels to those observed in wild-type and DTRtg mice (Fig. 2a). However, on day 7.5 of

Fig. 2 Effect of DC depletion on uterine NK cell differentiation. **a** Interleukin (*IL*)-15 and IL-15R transcripts at the implantation sites were detected by reverse transcriptase polymerase chain reaction (*RT-PCR*). Total RNA from implantation sites of wild-type, DCKO, and DTRtg mice on gestation days 5.5 and 7.5 was reversed-transcribed and PCR-amplified using IL-15- and IL-15R-specific primers. *M* DNA ladder. **b** Quantification of IL-15 and IL-15R mRNA expression. Density of each band at Gd 7.5 in the uterus was quantified using Scion Image software, and the ratio of bands of DCKO mice vs. WT and DTRtg mice was calculated. The *bars* denote the means for each group in which five mice/group were analyzed. *P<0.05; **P<0.01 as evaluated by nonparametric Mann–Whitney U test. **c** Schematic representation of the mouse pregnant uterus at gestation day 7.5. The region illustrated here is indicated for reference. *MD* mesometrial decidua, *NK* natural killer cells, *VZ* vascular zone, *EC* embryonic cavity, *AMD* anti-mesometrial decidua. *Top panel* Granules in uNK cells become dark pink after PAS staining. In the wild-type and DTRtg mice, uNK cells are abundant in the mesometrial decidua, while uNK cells are present in reduced numbers at DCKO implantation sites. Magnifications ×100 (*big panel*), ×200 (*top small panel*) Scale bars=50 μm. *Bottom panel* Perforin staining was performed using a specific antibody on implantation sites derived from wild-type, DCKO, and DTRtg mice on gestation day 7.5. Perforin-positive NK cells are located at the mesometrial decidua region. Magnifications ×100 (*big panel*), ×200 (*top small panel*) Scale bars=50 μm. **d** Quantification of PAS- and perforin-positive uNK cells in implantation sites of wild-type, DCKO, and DTRtg mice. PAS- and perforin-positive uNK cells were counted per square millimeter using magnification ×200. The *bars* denote the means for each group in which five mice/group were analyzed. *P< 0.05; **P<0.01 as evaluated by nonparametric Mann–Whitney U test

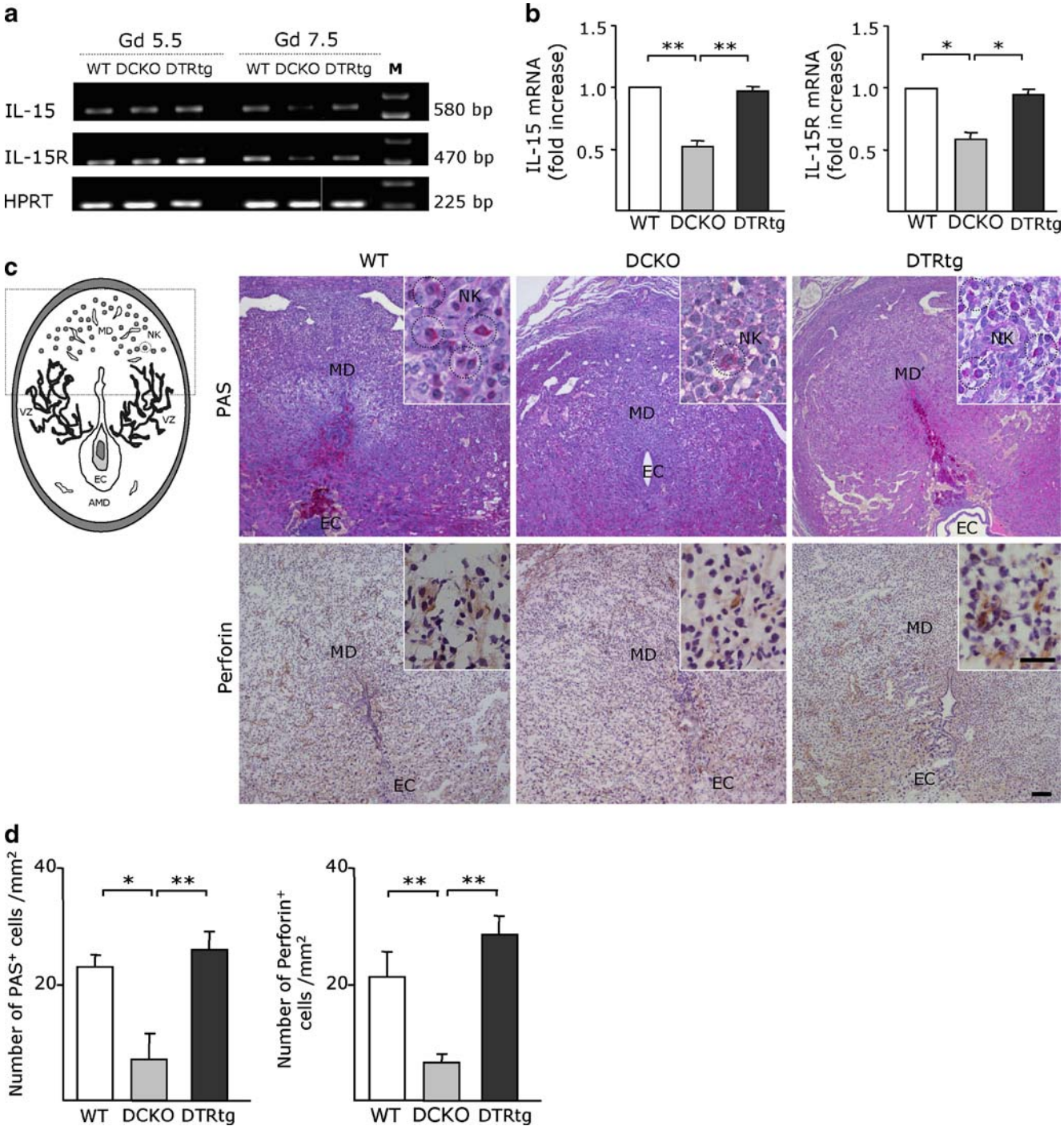

pregnancy, we observed a significantly decreased expression of IL-15 ($p<0.01$) and IL-15R ($p<0.05$) transcripts in DCKO compared to wild-type and DTRtg mice (Fig. 2b).

Our next aim was to determine whether DC depletion interferes with the accumulation of mature NK cells in the uterus. Here, we assessed the distribution of periodic-acid-Schiff (PAS; highlights NK glycogen-containing granules) and perforin-positive cells in DCKO, DTRtg, and wild-type mice. On gestation day 7.5, wild-type and DTRtg mice displayed numerous PAS- and perforin-positive cells throughout the uterine mesometrial decidua compartment (Fig. 2c), whereas four of five DC-deficient mice implantation sites contained fewer numbers of perforin-positive cells (Fig. 2c), suggesting that uNK cell differentiation is under the influence of DC-derived signals. Quantitative results (cells/mm^2) for PAS- and perforin-positive uNK cells in the uteri of wild-type and DCKO mice are displayed in Fig. 2d.

In line with these findings, we observed differences in vascular development between DC-depleted, DTRtg, and wild-type mice. Expression of endoglin and PECAM-1, two markers of endothelial cells within the vascular zone, was disarrayed in DC-depleted uteri compared with wild-type and DTRtg uteri (Fig. 3a). The typical endoglin and PECAM-1 pattern was not observable on Gd 7.5 in DC-depleted vascular zone.

Having the evidence that uterine cell proliferation in vitro occurs under the influence of uNK cell–DC interactions, we evaluated the stage of decidual cell proliferation by analyzing a well-established mitosis marker, phospho H3 histone (PHH3) by immunostaining. Results revealed a decreased number of proliferating cells in the decidua of DC-depleted ($9\pm4/mm^2$) compared to wild-type ($39.5\pm4/mm^2$) and DTRtg ($59.6\pm9/mm^2$) mice (Fig. 3b), indicating an impaired proliferation of decidual cells after DC depletion.

Identification of PITPβ as a DC-dependent protein involved during implantation

To identify novel DC-dependent proteins involved in implantation process, uterine tissues derived from DCKO, DTRtg, and wild-type mice from gestation day 5.5 were subjected to proteomic analysis. This approach identified a spot migrating with an apparent molecular mass of 35 kDa within uterine proteins from wild-type and DTRtg mice (Fig. 4a). The spot was excised from the gel and identified as phosphatidylinositol transfer protein β (PITPβ) by mass spectrometry (sequence coverage of 40.6%). Having iden-

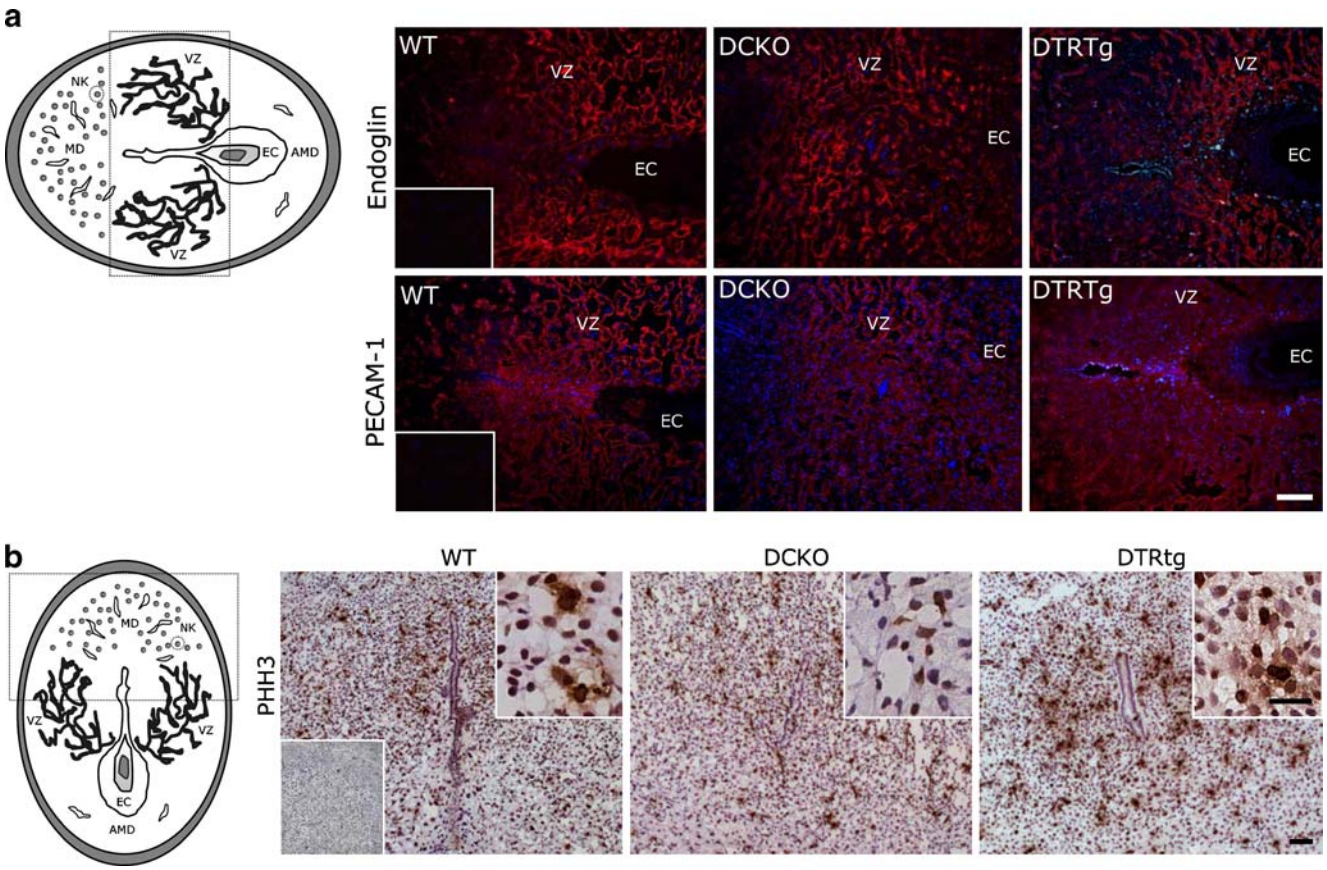

Fig. 3 Effect of DC depletion on vascular development. **a** Vascular organization at the implantation site on gestation day 7.5 of the wild-type, DC-depleted (*DCKO*), and DTRtg mice. Schematic diagram representing the pregnant uterus at gestation day 7.5. For reference, the vascular zone (*VZ*) has been squared in the diagram. The sections were immunostained with anti-endoglin (*top panels*) and anti-PECAM1 (*bottom panels*) antibodies. Worth noting is the disorganized vascular patterns in the DC-depleted mice (*top* and *bottom middle panels*) compared to the wild-type and DTRtg implantation sites. Magnification ×100, scale bar=50 μm. *Insets* show representative examples for the negative control immunostaining for endoglin and PECAM-1. **b** To assess cell proliferation in the decidua, implantation sites derived from wild-type, DCKO, and DTRtg mice at gestation day 7.5 were stained using an anti-phospho H3 histone (*PHH3*) antibody. The region of interest for this immunostaining has been highlighted in the diagram of the mouse pregnant uterus for reference. *MD* mesometrial decidua, *NK* natural killer cells, *VZ* vascular zone, *EC* embryonic cavity, *AMD* anti-mesometrial decidua. *Top panels* magnification ×100 and *bottom panels* magnification ×200, scale bars=50 μm. *Insets* show representative examples for the negative control immunostaining for PHH3

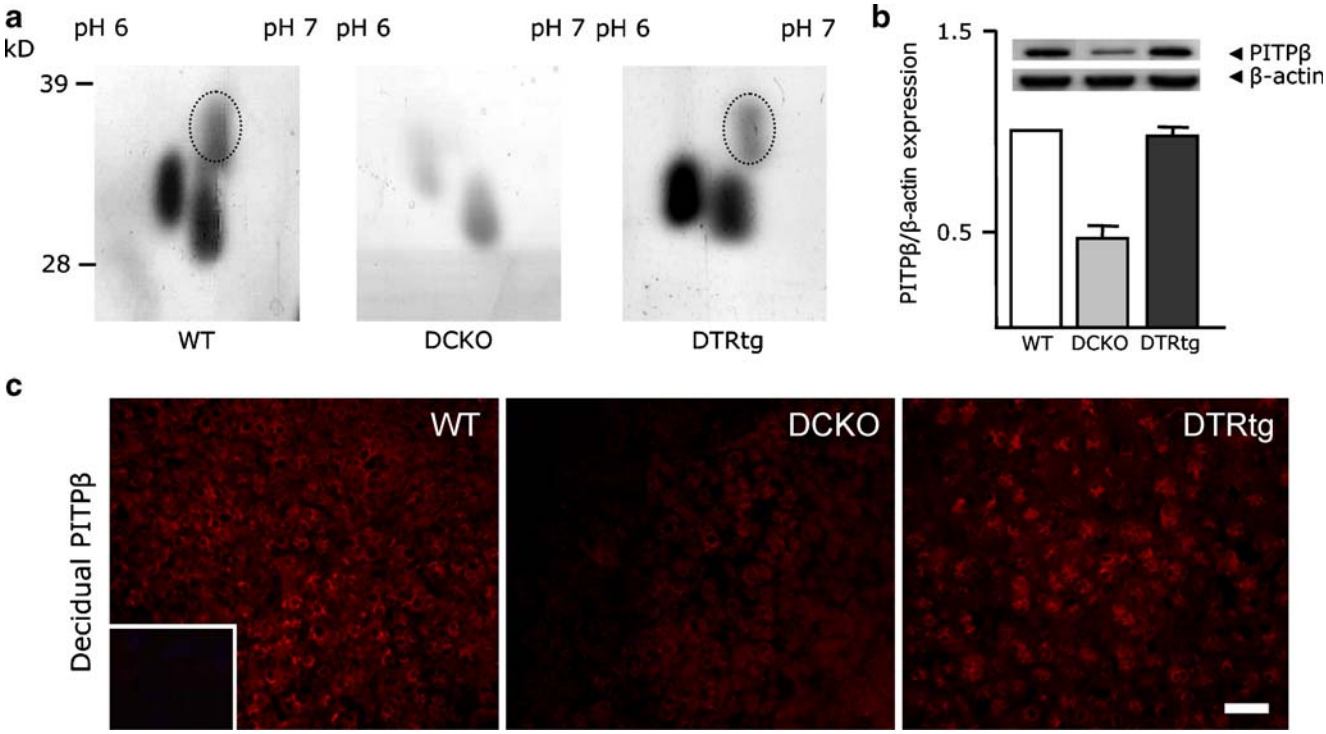

Fig. 4 Identification of PITPβ as a DC-dependent molecule potentially involved in the implantation process. **a** 2D gels of uterine proteins on gestation day 5.5 from wild-type, DC-depleted (*DCKO*), and DTRtg mice were run in parallel and *silver-stained*. The *encircled spots* at 35 kDa were excised and identified by MALDI-MS as phosphatidylinositol transfer protein beta (*PITP*β). **b** Immunoblot analysis of PITPβ expression in uterine tissues derived from wild-type, DC-depleted (*DCKO*), and DTRtg mice. The ratio of uterine PITPβ 35 kDa (*upper blot*) over β-actin 42 kDa (*lower blot*) expression on gestation day 5.5 was analyzed by Quantity One software (BioRad). **c** Immunolocalization of PITPβ expression on gestation days 5.5 in wild-type, DC-depleted (*DCKO*), and DTRtg mice. The photographs refer to the region squared on the schematic diagram of the pregnant uterus at gestation day 5.5. *MD* mesometrial decidua, *NK* natural killer cells, *VZ* vascular zone, *EC* embryonic cavity, *AMD* anti-mesometrial decidua. Magnification ×100, scale bars=50 μm

tified PITPβ as a novel DC-dependent protein, we reexamined uterine protein extracts on day 5.5 of gestation by immunoblotting analysis to determine whether PITPβ was differentially expressed. This was indeed the case, as a significant decrease in PITPβ uterine expression was observed on DC-depleted mice compared to wild-type and DTRtg mice (Fig. 4b). Furthermore, immunostaining showed PITPβ expression in the mesometrial decidua on gestation day 5.5 (Fig 4c). However, we observed a decrease on the PITPβ expression on DC-depleted mice compared to DTRtg and wild-type mice. The immunoreactivity of PITPβ matched the results obtained with immunoblotting analysis.

Abnormalities in placental development after DC depletion

Having identified PITPβ using a proteomic approach, we next examined whether loss of DC during the implantation process could influence placental development. It is known that PITPβ plays a main role during blastocyst activation, placental development, trophoblast differentiation/invasion, and embryonic development [26–30]. First of all, cytokeratin immunostaining was used to evaluate the integrity of the trophoblast cell lineage. As shown in Fig. 5a, the number of trophoblast cells was diminished. The embryonic cavity in DC-depleted implantation sites was diffuse compared to implantation sites in DTRtg and wild-type mice, indicating abnormalities in early placental development upon DC depletion.

To assess whether the trophoblast differentiation was also impaired, we examined two hallmarks of trophoblast differentiation, PLF and PL-1 [31]. As shown in Fig. 5b, trophoblast giant cells derived from DCKO mice displayed a decreased expression of PL-1 and PLF compared to DTRtg and wild-type mice on Gd 10.5. Similar results were obtained when progesterone levels were evaluated on Gd 13.5 in DC-depleted, DTRtg, and wild-type mice. DCKO female mice displayed significantly lower progesterone levels when compared to DTRtg and wild-type mice (Table 2). Furthermore, placentas obtained from DT-treated WT C57BL/6 females displayed abundant trophoblast giant cells with normal morphology and well-constituted spongiotrophoblast and labyrinthine layers. Likewise, placentas from PBS-treated DTRtg females also had a normal appearance, indicating the absence of intrinsical dysregulations in placental development due to differences in genetic background between WT and transgenic mice (Fig. 5c). However, hematoxylin and eosin (H&E)

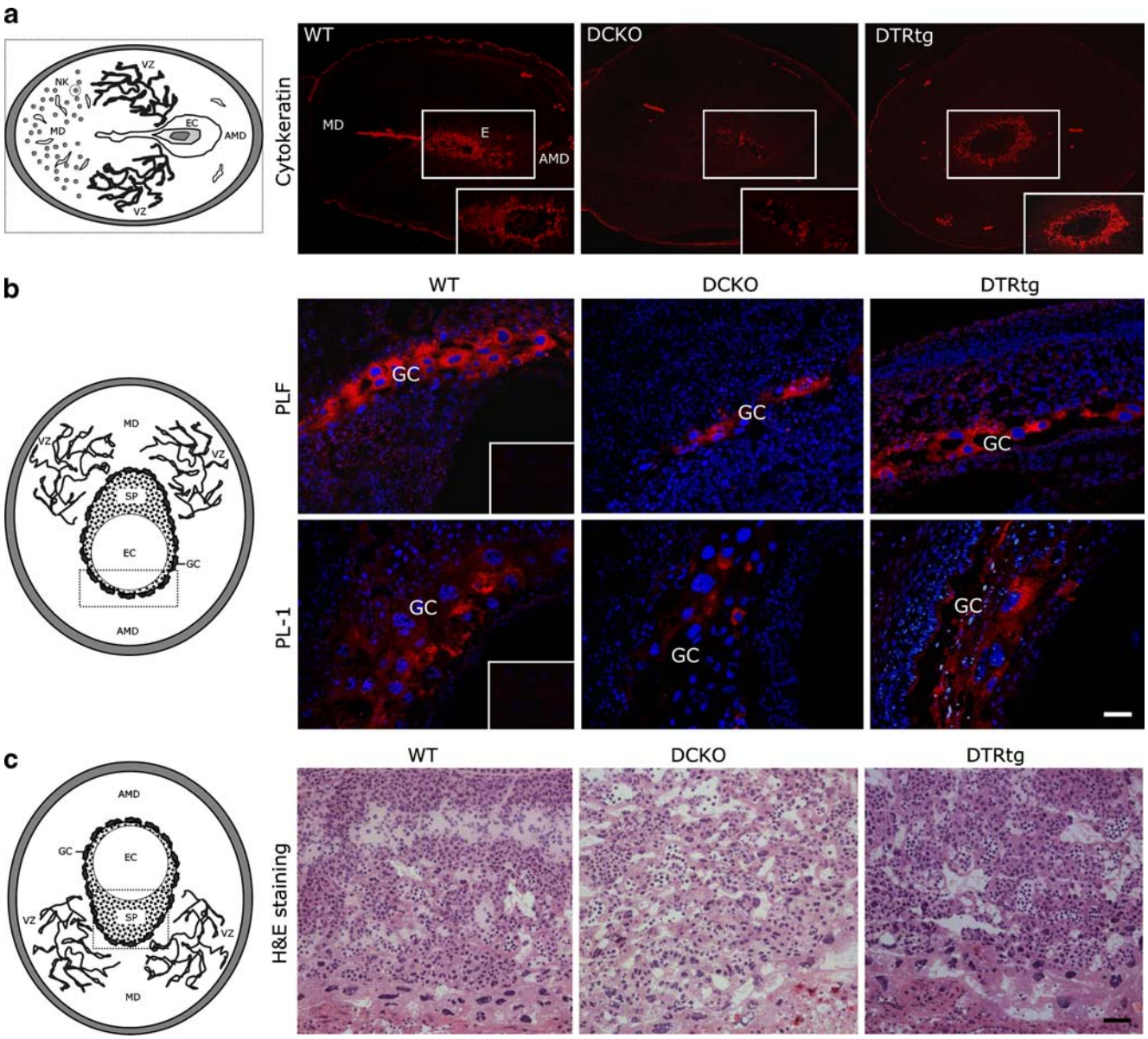

Fig. 5 Abnormalities in placental development after DC depletion. **a** Expression of cytokeratin (*CK*; *appearing in red*) which reveals integrity of cells belonging to the trophoblast lineage was assessed on gestation day 7.5 in implantation site sections derived from wild-type (*left panel*), DC-depleted (*middle panel*), and DTRtg mice (*right panel*), magnification ×50. *Inset* shows embryonic trophoblasts, magnification ×100. **b** Characterization of trophoblast differentiation on gestation day 10.5 in wild-type, DC-depleted (*DCKO*), and DTRtg mice. Diagram representing the pregnant uterus on gestation day 10.5 showing the region illustrated in the photographs for reference. *MD* mesometrial decidua, *VZ* vascular zone, *EC* embryonic cavity, *SP* spongio zone, *GC* giant cells, *AMD* anti-mesometrial decidua. Eight-micron cryosections of the tissue were prepared and immunostained with anti-proliferin (*PLF*, *top panels*) and placental lactogen 1 (*PL-1*, *bottom panels*), magnification ×200. *Insets* show representative examples for the negative control immunostaining for PLF and PL-1. Scale bar=50 μm. **c** Hematoxylin and eosin staining (*H&E*) of the placental zone from wild-type, DCKO, and DTRtg implantation sites at gestation day 10.5. Magnification ×100; *scale bar* 50 μm

staining revealed several anomalies in placental architecture in DCKO mice, including a marked hypocellularity of the placental spongiotrophoblast and labyrinth, as well as decreased amounts of trophoblast giant cells (Fig. 5c). These results suggest that DC could be involved in the regulation of trophoblast development and placental function during pregnancy.

Discussion

It is widely believed that dendritic cells are critical for feto-maternal tolerance [14, 32]. Although several studies have demonstrated that DC are highly potent pregnancy regulators, experimental evidence for a unique in vivo function of DC has been lacking. In this study, we used the DCKO

Table 2 Progesterone levels in mouse sera following DT administration

Group	Gestation day	Progesterone (ng/ml)
Wild-type mice	13.5	68.55±4.43
DCKO		48.68±6.08*
DTRtg		75.25±6.32

Quantification of progesterone levels in serum from wild-type, DTRtg, and DC-depleted (DCKO) mice by ELISA at gestation day 13.5 (n=5, per group). Results are expressed as mean±SEM.
*P<0.01 (as evaluated by non-parametric Mann–Whitney U test)

system that allows to inducibly deplete CD11c$^+$ DC in vivo during implantation. The series of experiments reported herein strongly suggests that DC play a role during implantation in mice since DC depletion impairs uNK differentiation and vascular and placental development. These data support the important role played by DC in the orchestration of events leading to the establishment and maintenance of pregnancy.

After implantation, uterine stromal cells differentiate into decidual cells. These specialized cells control the environment in which the embryo develops [33]. The decidualization process is accompanied by an increase of the numbers of uterine CD11c$^+$ cells, as we have previously described [14]. In this study, we showed that DC depletion on Gd 4.5 results in failure of the implantation process, affecting the breeding efficiency as well. Our results therefore extend the previously reported by suggesting that CD11c$^+$ DC seem to be important for a successful implantation outcome.

We first examined the effect of DC depletion on the uNK cell population, considering that during mouse pregnancy, these cells accumulate on the mesometrial decidua and play a central role in decidualization. DT treatment markedly reduced uNK cell recruitment and development, most likely reflecting that NK cell accumulation depends on DC signaling. Thus, expression of the major cytokine regulating the uterine NK cell lineage, IL-15, was decreased after DC depletion. IL-15 synthesis has been detected in the uteroplacental unit of mice and human [7, 25], and its production seems to be restricted to the decidua during mouse pregnancy where local IL-15 synthesis regulates the development of uNK cells from their precursors [34, 35]. Interestingly, recent data have revealed a role for IL-15-expressing CD11c$^+$ DC during NK cell priming [36]. IL-15 expression by many cells in the decidual microenvironment including other leukocytes and epithelial cells [8, 9] cannot be disregarded. However, the key role of CD11c$^+$ DC for NK cell development is likely attributable to their unique ability to create a locally confined niche of intimate NK cell/DC contact in the decidualized uterus [24] and to their immediate up-regulation of both IL-15 and IL-15R expression during implantation. Our data indicate that the IL-15/IL-15R system is a DC-dependent signaling complex and regulates crucial aspects of NK cell differentiation. Interestingly, while in the present study wild-type and DTRtg mice NK cells start differentiating into granulated uNK cells that express perforin as described before [12, 37], NK cell differentiation is negatively affected by disruption of DC signaling.

Uterine NK cells have been proposed to participate in the regulation of vascular development at the implantation sites [12, 38–40]. Mouse strains lacking uNK cells show common histopathology, including acellular and edematous decidua basalis and deficient uterine spiral artery remodeling [39]. These findings imply that normal uNK cell functions during pregnancy are to interact with and support the growth of stromal cells committed to decidual differentiation and to trigger events that culminate in pregnancy-induced vascular modification [12]. Moreover, disruptions in NK cell function have been postulated to cause pregnancy-associated diseases, such us preeclampsia, intrauterine growth restriction, and early pregnancy failure [5, 41]. Not surprisingly, the NK cell differentiation deficiency in DCKO uteri was also associated with a disorganized decidual vasculature and impaired decidual cell proliferation. In our recent in vitro study, we have observed that NK-DC cross talk is needed during decidual cell proliferation [21], and this could represent a possible explanation for the decrease of uterine proliferation observed on DCKO mice. Whether DC signaling affects vascular development directly and/or indirectly trough NK cell and/or decidual cell mediators remains to be determined.

By means of the proteomic approach described in this study, it was possible to identify PITPβ as a novel DC-dependent protein during implantation. PITP is a ubiquitous cytosolic domain involved in transport of phospholipids from their site of synthesis in the endoplasmic reticulum and Golgi to other cell membranes [42]. Interestingly, it has been shown that PITPs play an important role during in vivo pre-implantation embryo development, as oviductal epithelia increase the expression of PITPs before the embryo implants [43]. Lee et al. [43] hypothesized that epithelial cells in the oviduct, where fertilization and early embryo implantation is taking place, secrete PITP for enhancing embryo development.

A significantly decreased expression of PITPβ has been shown in DCKO mice during this study. As PITPβ can participate in the transport of phosphatidylinositol-4,5-bisphosphate (PIP2) precursors and has been shown to act as a cofactor for PIP2 production [44–46], a reduced expression of PITPβ might directly influence the downstream PI3K/Akt signaling pathway and could thus affect processes depending on it, including blastocyst activation, placental development, trophoblast differentiation, trophoblast invasion, and embryonic development [26–30]. Thus, the PITPβ down-regulation could be one of the explanations for impaired implantation and placentation processes in DC-depleted mice. We further show that PITPβ expression depends on DC

signaling, since DTRtg implantation sites showed a similar expression compared to the wild-type group. However, the question as to how the impact of DC absence on PITPβ expression is mediated remains to be elucidated.

In addition, some aspects of the trophoblast cell differentiation process occur in DC-depleted mice, but with decreased efficiency. Indeed, our observations showing differential expression of PLF and PL-1 as markers of placental development in DC-depleted mice support the notion that DC depletion affects via PITPβ signaling the trophoblast integrity in early embryo development.

Although it is clear that deficiencies on the implantation sites can be directly attributed to the loss of the $CD11c^+$ DC expressing populations, the underlying mechanisms remain unresolved. Because DCKO mice lose significant numbers of their myeloid, lymphoid, and to a lesser extent, their plasmacytoid DC simultaneously, the individual contribution of each of these DC subsets remains unclear. Further studies will be required to dissect the role of individual $CD11c^+$ populations in implantation outcome as well as the underlying mechanisms involved. However, this study has unequivocally demonstrated that normal numbers of $CD11c^+$ DC are required for a successful implantation outcome.

Acknowledgments This work was supported by research grants from the Charité (AF-2007-011) to S.M.B. G.B. and R.C-R. received a scholarship from the German Student Exchange Program (Deutscher Akademischer Austauschdienst). S.M.B is a fellow of the Habilitation program at the Charité, University Medicine Berlin. P.C.A. and S.M. B. are part of the EMBIC Network of Excellence, co-financed by the European Commission throughout the FP6 framework program Life Science, Genomics and Biotechnology for Health.

Author contributions G.K. performed all the experiments and contributed to manuscript writing; V.S. designed and performed proteomics experiments. P.F., G.B., and P.M. performed histological analysis and animal experiments; R.C-R. and F.R. assisted with the PCR experiments; I.C. and M.M. assisted with MALDI-MS experiments; B.F.K and N.F provided advice, P.C.A. contributed with reagents and S.M.B. supervised the work, designed the experiments and wrote the manuscript.

References

1. Aluvihare VR, Kallikourdis M, Betz AG (2005) Tolerance, suppression and the fetal allograft. J Mol Med 83.2:88–96 (Feb)
2. Carson DD, Bagchi I, Dey SK, Enders AC, Fazleabas AT, Lessey BA, Yoshinaga K (2000) Embryo implantation. Dev Biol 223.2: 217–237 (Jul 15)
3. Norwitz ER, Schust DJ, Fisher SJ (2001) Implantation and the survival of early pregnancy. N Engl J Med 345.13:1400–1408 (Nov 8)
4. Lydon JP, DeMayo FJ, Funk CR, Mani SK, Hughes AR, Montgomery CA Jr, Shyamala G, Conneely OM, O'Malley BW (1995) Mice lacking progesterone receptor exhibit pleiotropic reproductive abnormalities. Genes Dev 9.18:2266–2278 (Sep 15)
5. Moffett-King A (2002) Natural killer cells and pregnancy. Nat Rev Immunol 2.9:656–663 (Sep)
6. Croy BA, Esadeg S, Chantakru S, van den Heuvel M, Paffaro VA, He H, Black GP, Ashkar AA, Kiso Y, Zhang J (2003) Update on pathways regulating the activation of uterine natural killer cells, their interactions with decidual spiral arteries and homing of their precursors to the uterus. J Reprod Immunol 59.2:175–191 (Aug)
7. Verma S, Hiby SE, Loke YW, King A (2000) Human decidual natural killer cells express the receptor for and respond to the cytokine interleukin 15. Biol Reprod 62.4:959–968 (Apr)
8. Shinozaki M, Hirahashi J, Lebedeva T, Liew FY, Salant DJ, Maron R, Kelley VR (2002) IL-15, a survival factor for kidney epithelial cells, counteracts apoptosis and inflammation during nephritis. J Clin Invest 109.7:951–960 (Apr)
9. Waldmann TA, Dubois S, Tagaya Y (2001) Contrasting roles of IL-2 and IL-15 in the life and death of lymphocytes: implications for immunotherapy. Immunity 14.2:105–110 (Feb)
10. Ain R, Canham LN, Soares MJ (2003) Gestation stage-dependent intrauterine trophoblast cell invasion in the rat and mouse: novel endocrine phenotype and regulation. Dev Biol 260.1:176–190 (Aug 1)
11. Ashkar AA, Di Santo JP, Croy BA (2000) Interferon gamma contributes to initiation of uterine vascular modification, decidual integrity, and uterine natural killer cell maturation during normal murine pregnancy. J Exp Med 192.2:259–270 (Jul 17)
12. Croy BA, He H, Esadeg S, Wei Q, McCartney D, Zhang J, Borzychowski A, Ashkar AA, Black GP, Evans SS, Chantakru S, van den Heuvel M, Paffaro VA Jr, Yamada AT (2003) Uterine natural killer cells: insights into their cellular and molecular biology from mouse modelling. Reproduction 126.2:149–160 (Aug)
13. Guimond MJ, Luross JA, Wang B, Terhorst C, Danial S, Croy BA (1997) Absence of natural killer cells during murine pregnancy is associated with reproductive compromise in TgE26 mice. Biol Reprod 56.1:169–179 (Jan)
14. Blois SM, Alba Soto CD, Tometten M, Klapp BF, Margni RA, Arck PC (2004) Lineage, maturity, and phenotype of uterine murine dendritic cells throughout gestation indicate a protective role in maintaining pregnancy. Biol Reprod 70.4:1018–1023 (Apr)
15. Haimovici F, Anderson DJ (1993) Cytokines and growth factors in implantation. Microsc Res Tech 25.3:201–207 (Jun 15)
16. Blois SM, Ilarregui JM, Tometten M, Garcia M, Orsal AS, Cordo-Russo R, Toscano MA, Bianco GA, Kobelt P, Handjiski B, Tirado I, Markert UR, Klapp BF, Poirier F, Szekeres-Bartho J, Rabinovich GA, Arck PC (2007) A pivotal role for galectin-1 in fetomaternal tolerance. Nat Med 13(12):1450–1457 (Dec)
17. Laskarin G, Kämmerer U, Rukavina D, Thomson AW, Fernandez N, Blois SM (2007) Antigen-presenting cells and materno-fetal tolerance: an emerging role for dendritic cells. Am J Reprod Immunol 58(3):255–67 (Sep)
18. Ferlazzo G, Pack M, Thomas D, Paludan C, Schmid D, Strowig T, Bougras G, Muller WA, Moretta L, Munz C (2004) Distinct roles of IL-12 and IL-15 in human natural killer cell activation by dendritic cells from secondary lymphoid organs. Proc Natl Acad Sci U S A 101.47:16606–16611 (Nov 23)
19. Yu Y, Hagihara M, Ando K, Gansuvd B, Matsuzawa H, Tsuchiya T, Ueda Y, Inoue H, Hotta T, Kato S (2001) Enhancement of human cord blood CD34+ cell derived NK cell cytotoxicity by dendritic cells. J Immunol 166:1590–1600
20. Piccioli D, Sbrana S, Melandri E, Valiante N (2002) Contact-dependent stimulation and inhibition of dendritic cells by natural killer cells. J Exp Med 195:335–341
21. Blois SM, Barrientos G, Garcia MG, Orsal AS, Tometten M, Cordo-Russo R, Klapp BF, Santoni A, Fernandez N, Terness P, Arck PC (2008) Interaction between dendritic cells and natural killer cells during pregnancy in mice. J Mol Med (doi:10.1007/s00109-008-0342-2)
22. Jung S, Unutmaz D, Wong P, Sano G, De los Santos K, Sparwasser T, Wu S, Vuthoori S, Ko K, Zavala F, Pamer EG, Littman DR, Lang RA (2002) In vivo depletion of CD11c(+) dendritic cells abrogates

priming of CD8(+) T cells by exogenous cell-associated antigens. Immunity 17.2:211–220 (Aug)
23. Probst HC, Tschannen K, Odermatt B, Schwendener R, Zinkernagel RM, Van Den Broek M (2005) Histological analysis of CD11c-DTR/GFP mice after in vivo depletion of dendritic cells. Clin Exp Immunol 141.3:398–404 (Sep)
24. Kammerer U, Eggert AO, Kapp M, McLellan AD, Geijtenbeek TB, Dietl J, van Kooyk Y, Kampgen E (2003) Unique appearance of proliferating antigen-presenting cells expressing DC-SIGN (CD209) in the decidua of early human pregnancy. Am J Pathol 162.3:887–896 (Mar)
25. Ye W, Zheng LM, Young JD, Liu CC (1996) The involvement of interleukin (IL)-15 in regulating the differentiation of granulated metrial gland cells in mouse pregnant uterus. J Exp Med 184.6: 2405–2410 (Dec 1)
26. Wang H, Dey S (2006) Roadmap to embryo implantation: clues from mouse models. Nat Rev Genet 7.3:185–199
27. Yang Z, Tschopp O, Hemmings-Mieszczak M, Feng J, Brodbeck D, Perentes E, Hemmings B (2003) Protein kinase B alpha/Akt1 regulates placental development and fetal growth. J Biol Chem 278:32124–32131
28. Riley J, Moley K (2006) Glucose utilization and the PI3-K-pathway: mechanisms for cell survival in preimplantation embryos. Reproduction 131:823–835
29. Qiu Q, Yang M, Tsang B, Gruslin A (2004) EGF-induced trophoblast secretion of MMP-9 and TIMP-1 involves activation of both PI3K and MAPK signalling pathways. Reproduction 128:355–363
30. Kamei T, Jones S, Chapman B, McGonigle K, Dai G, Soares M (2002) The phosphatidylinositol 3-Kinase/Akt signaling pathway modulates the endocrine differentiation of trophoblast cells. Mol Endocrinol 16(7):1469–1481
31. Faria TN, Soares MJ (1991) Trophoblast cell differentiation: establishment, characterization, and modulation of a rat trophoblast cell line expressing members of the placental prolactin family. Endocrinology 129.6:2895–2906 (Dec)
32. Blois SM, Kammerer U, Soto CA, Tometten MC, Shaikly V, Barrientos G, Jurd R, Rukavina D, Thomson AW, Klapp BF, Fernandez N, Arck PC (2007) Dendritic cells: key to fetal tolerance? Biol Reprod 77.4:590–598 (Oct)
33. Parr MB, Parr EL (1989) Immunohistochemical investigation of secretory component and immunoglobulin A in the genital tract of the female rat. J Reprod Fertil 85.1:105–113 (Jan)
34. Ashkar AA, Black GP, Wei Q, He H, Liang L, Head JR, Croy BA (2003) Assessment of requirements for IL-15 and IFN regulatory factors in uterine NK cell differentiation and function during pregnancy. J Immunol 171.6:2937–2944 (Sep 15)
35. Barber EM, Pollard JW (2003) The uterine NK cell population requires IL-15 but these cells are not required for pregnancy nor the resolution of a Listeria monocytogenes infection. J Immunol 171.1:37–46 (Jul 1)
36. Lucas M, Schachterle W, Oberle K, Aichele P, Diefenbach A (2007) Dendritic cells prime natural killer cells by trans-presenting interleukin 15. Immunity 26.4:503–517 (Apr)
37. Burnett TG, Hunt JS (2000) Nitric oxide synthase-2 and expression of perforin in uterine NK cells. J Immunol 164.10:5245–5250 (May 15)
38. Croy BA, Luross JA, Guimond MJ, Hunt JS (1996) Uterine natural killer cells: insights into lineage relationships and functions from studies of pregnancies in mutant and transgenic mice. Nat Immunol 15.1:22–33
39. Croy BA, Ashkar AA, Foster RA, DiSanto JP, Magram J, Carson D, Gendler SJ, Grusby MJ, Wagner N, Muller W, Guimond MJ (1997) Histological studies of gene-ablated mice support important functional roles for natural killer cells in the uterus during pregnancy. J Reprod Immunol 35.2:111–133 (Nov 15)
40. Wang C, Tanaka T, Nakamura H, Umesaki N, Hirai K, Ishiko O, Ogita S, Kaneda K (2003) Granulated metrial gland cells in the murine uterus: localization, kinetics, and the functional role in angiogenesis during pregnancy. Microsc Res Tech 60.4:420–429 (Mar 1)
41. Croy BA, Ashkar AA, Minhas K, Greenwood JD (2000) Can murine uterine natural killer cells give insights into the pathogenesis of preeclampsia? J Soc Gynecol Investig 7.1:12–20 (Jan–Feb)
42. Cockcroft S, Carvou N (2007) Biochemical and biological functions of class I phosphatidylinositol transfer proteins. Biochim Biophys Acta 1771.6:677–691 (Jun)
43. Lee KF, Kwok KL, Chung MK, Lee YL, Chow JF, Yeung WS (2005) Phospholipid transfer protein (PLTP) mRNA expression is stimulated by developing embryos in the oviduct. J Cell Biochem 95.4:740–749 (Jul 1)
44. Cunningham E, Thomas G, Ball A, Hiles I, Cockcroft S (1995) Phosphatidylinositol transfer protein dictates the rate of inositol trisphosphate production by promoting the synthesis of PIP2. Curr Biol 5.7:775–783
45. Martin T (1995) Intracellular signalling. New directions for phosphatidylinositol transfer. Curr Biol 5.9:990–992
46. Panaretou C, Domin J, Cockcroft S, Waterfield M (1997) Characterization of p150, an adaptor protein for the human phosphatidylinositol (PtdIns) 3-kinase. Substrate presentation by phosphatidylinositol transfer protein to the p150.Ptdins 3-kinase complex. J Biol Chem 272.4:2477–2485